Observation of a Fast Electron Beam Emitted along the Surface of a Target Irradiated by Intense Femtosecond Laser Pulses

Y. T. Li,[1] X. H. Yuan,[1,2] M. H. Xu,[1] Z. Y. Zheng,[1] Z. M. Sheng,[1] M. Chen,[1] Y. Y. Ma,[1] W. X. Liang,[1] Q. Z. Yu,[1] Y. Zhang,[1] F. Liu,[1] Z. H. Wang,[1] Z. Y. Wei,[1] W. Zhao,[2] Z. Jin,[1] and J. Zhang[1,*]

[1]*Beijing National Laboratory for Condensed Matter Physics, Institute of Physics, Chinese Academy of Sciences, Beijing 100080, China*

[2]*State Key Laboratory of Transient Optics Technology, Chinese Academy of Sciences, Xi'an 710068, China*

(Received 10 July 2005; revised manuscript received 15 February 2006; published 27 April 2006)

A novel fast electron beam emitting along the surface of a target irradiated by intense laser pulses is observed. The beam is found to appear only when the plasma density scale length is small. Numerical simulations reveal that the electron beam is formed due to the confinement of the surface quasistatic electromagnetic fields. The results are of interest for potential applications of fast electron beams and deep understanding of the cone-target physics in the fast ignition related experiments.

DOI: 10.1103/PhysRevLett.96.165003 PACS numbers: 52.38.Kd, 52.38.Fz

The generation and transport of fast electrons are fundamental processes in the intense laser interactions with plasmas [1–6]. They determine a number of secondary processes such as high energy ion [7–10], hard x-ray [11], and neutron emissions [12]. One of the potential applications of fast electrons is the fast ignitor scheme [13] for laser confinement fusion. In this scheme a collimated fast electron beam generated by a short laser pulse could be used to rapidly heat a precompressed fuel pellet to ignition. Recently a reentrant cone concept has been proposed to keep the path of the intense heating laser pulse free of the large scale coronal plasma surrounding the compressed core. The integrated cone or shell experiments performed at Osaka University have shown a 1000-fold increase in neutron yield [14,15]. Particle-in-cell (PIC) simulations have predicted the twofold roles of the hollow cone, the refocusing of laser light by the conical wall and the guiding of fast electrons along the inner surface of the cone to the tip [16]. The first one agrees with the measured enhancement of the optical emission and fast electrons from the rear side of a single cone target [17,18]. Such measurements also support the possible guiding of fast electrons along the inner cone surface. However, the evidences are indirect and weak because: (i) one cannot distinguish the guiding of fast electrons from the refocusing of laser light. The measured enhancement may be explained by any one or both; (ii) one also cannot distinguish the fast electrons, initially generated on the cone sidewall (then flowed to the tip along the inner surface), from those directly generated at the tip. Both of them contribute to the enhanced signals recorded on the detectors. Recent cone-target experiments at the Rutherford [19] and LULI laboratories [20] did not show significant cone-guiding effects. Therefore, it is necessary to carry out simple and clean experiments to understand the generation and transport of fast electrons with a cone target.

This Letter presents an experimental observation of a collimated fast electron beam along the target surface in intense laser interactions with planar foils at large incident angles. It is found that this beam emission strongly depends on the preplasma conditions, while weakly depends on the laser polarizations and target materials. Our PIC simulations suggest that the electron beam is formed due to the confinement of the surface quasistatic electromagnetic fields. The results shed light on the cone-target physics and should be of interest for applications of fast electron beams.

The experiments were carried out using the Xtreme Light II (XL-II) laser system at the Institute of Physics, Chinese Academy of Sciences. The laser system can produce a p-polarized pulse with an energy up to 0.6 J in 30 fs at 800 nm. The amplified spontaneous emission was measured to be $\sim 10^{-5}$. The laser pulse was focused by an $f/3.5$ off-axis parabolic mirror onto a 30 μm thick aluminum foil. The focal spot size was monitored by an x-ray pinhole or a knife-edge camera. The diameter of the focus was ~ 10 μm at the full width at half maximum (FWHM). The angular distributions of fast electrons were measured by an array of sandwiched imaging plate (IP) stacks. The stack array radially surrounded the laser focus in the plane of laser incidence. The distance from the focus to each stack was 5.5 cm. The 2π radial angle in the plane of the laser incidence was almost fully covered by the IP stack array except for an angle of 25° left for laser entrance in front of the target. The electron energy ranges were chosen by the aluminum filters in front of the first IP layer and those inserted in adjacent layers. A magnetic spectrometer with 1000 G permanent magnets was used to measure the electron energy spectrum. The energy spectrum was also recorded by the calibrated IP [21].

Figures 1(a)–1(c) show the angular distributions of the fast electrons in the incident plane at a laser intensity of $1\text{–}2 \times 10^{18}$ W/cm^2. Here 0° corresponds to the laser incident direction. The data have been rescaled to 100 for the maximum. Some fast electrons are emitted between the target normal and the laser specular directions in front of

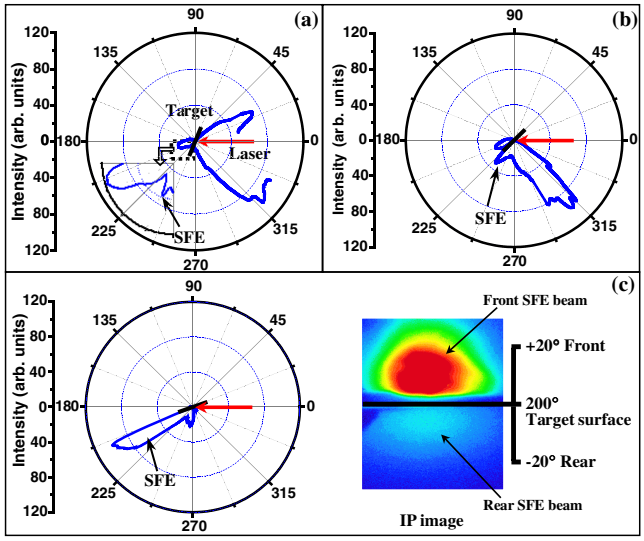

FIG. 1 (color online). The angular distributions of the fast electrons with energies >300 keV for three incidence angles of 22.5° (a), 45° (b), and 70° (c), respectively. An inset with enlarged scale is also given in (a) to show the surface electron beam more clearly. The right part of (c) shows the IP image of the fast electron beam emitted close to the target surface.

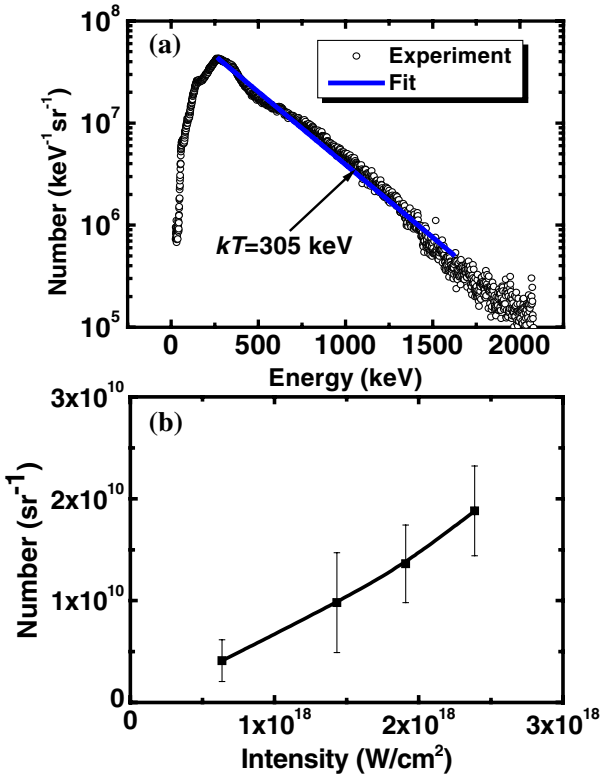

FIG. 2 (color online). (a) The energy spectrum of the SFE beam at the incidence angle 70°, detected at 10° relative to the front target surface; (b) The dependence of the fast electron number contained in the beam on the laser intensity.

the target, similar to previous observations by different groups [22–24]. The most striking aspect of our measurements is the presence of a novel fast electron beam emitted along the front target surface, marked as ''surface fast electron (SFE)'' in the figures. The SFE beam becomes increasingly pronounced when increasing the laser incident angle [25]. The intensity of the SFE beam at the incident angle 70° reaches ~5 times higher than that of the beam close to the specular direction. It is well reproducible and collimated, with a cone angle less than 15° (FWHM). The single-shot energy spectrum of the SFE measured at 10° with respect to the front target surface is shown in Fig. 2(a). The distribution peaks at about 290 keV and the detectable maximum energy approaches 2000 keV. The effective temperature, kT, is 305 keV, obtained by fitting the spectrum with an exponential decay. The dependence of the numbers of fast electrons with energies >300 keV per sterad, measured within the SFE beam, on the laser intensity are shown in Fig. 2(b). The electron numbers are approximately proportional to the laser intensity.

The peak of the transmitted beam behind the target does not coincide with the laser propagation direction, but is deflected towards the rear target surface. This deflection becomes much pronounced for the large incidence angles. The transmitted electron beam for 70° is emitted almost parallel with the rear surface [marked as ''Rear SFE beam'' in the IP image in Fig. 1(c)].

The fractions of the SFE and the transmitted fast electrons, given by $f_{se} = N_{se}/N_{tot}$ and $f_{te} = N_{te}/N_{tot}$, respectively, where N_{se} denotes the number of fast electrons along the front surface, N_{te} the number of all transmitted electrons within 1π angle behind the target, and N_{tot} the number of total ejected electrons found in both sides of the target, are listed in Table I. The uncertainty comes from the shot-to-shot fluctuations from 3–5 shots. The results indicate that, with the increase of laser incidence angles, the fraction of front SFE f_{se} increases, while the transmitted fraction f_{te} decreases. For the 70° case, f_{se} increases up to about 60%, while f_{te} almost reduces to the noise level.

To understand the measurements, numerical simulations have been conducted with our 2D fully relativistic PIC code. Figure 3(a) shows the simulation geometry. In the simulations, a p-polarized laser pulse with an irradiance of $2–5 \times 10^{18}$ W/cm^2 is incident at 70° onto a $4\lambda_0$ thick plasma slab with an initial density of $8n_c$, where n_c and λ_0 are the critical density and the laser wavelength, respectively. The diameter of the laser focus is $10\lambda_0$. The laser electric field is in the Y direction.

TABLE I. The ratios of the front SFE and the transmitted fast electrons to the total fast electrons.

Incident angle	f_{se}	f_{te}
22.5°	<6%	20%–28%
45°	17%–28%	8%–16%
60°	40%–45%	<6%
70°	50%–65%	<5%

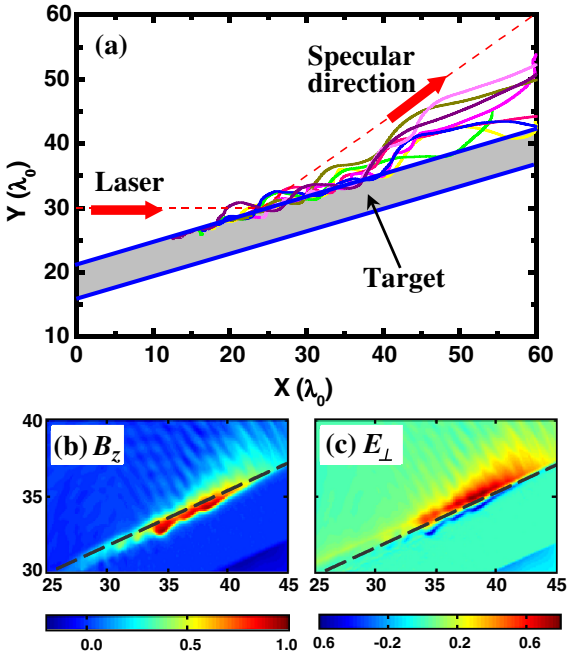

FIG. 3 (color online). (a) 2D-PIC simulation geometry and selected fast electron trajectories along the front target surface; (b) and (c) show snapshots of the distributions of the quasistatic magnetic field B_z and electric field $E_\perp$, respectively. The dashed black lines in (b) and (c) mark the initial front target surface. The fields are normalized by $m\omega_0 c/e$.

Selected trajectories of fast electrons at the front target surface are illustrated in Fig. 3(a). A large number of fast electrons in the focus move along the target surface in an oscillating form. This novel phenomenon is due to the confinement of surface quasistatic magnetic and electric fields. At the early stage, when the fast electrons generated by $\boldsymbol{J} \times \boldsymbol{B}$ heating or vacuum heating in a plasma with a steep density gradient are accelerated into the target bulk, a quasistatic magnetic field will be induced by the fast electron current around the front surface. Simultaneously, a charge separation field is generated because some electrons are pulled out into vacuum by the laser electric field. Figures 3(b) and 3(c) show the distributions of the quasistatic magnetic field B_z, and the electrostatic field $E_\perp$ around the laser focus, respectively. The B_z field is positive, directing the readers out of the paper plane. $E_\perp$ is the electric field perpendicular to the target surface in the X-Y plane. The fields are normalized by the incident laser amplitude. Part of the fast electrons generated in the interaction will be reflected back to the vacuum by B_z. However, the negative $E_\perp$, whose peak position slightly shifts to the vacuum relative to that of the B_z, will push them back to target again. The push-pull processes lead to a fast electron current along the surface, which in turn enhances the surface magnetic field component. Therefore, a fast electron flow along the target surface is produced self-consistently. After running away from the focus, the electrons form the fast electron beam along the front target surface.

The oscillations of the fast electrons along the surface are very similar to the electron motion in a laser self-focusing channel, where electrons make betatron oscillations forced by the self-generated quasistatic electric and magnetic fields [26,27]. Some electrons in the channel can gain significant energy from the laser wave when their oscillation frequency is resonant with the laser frequency. In our simulations we identify a similar process for some energetic electrons emitted along the front surface [28]. When changing the laser intensity, similar intensity dependence for the surface electron number as shown in Fig. 2(b) is found in our numerical simulations.

The deflection of the transmitted electron beam to the rear target surface observed in the experiments can also be explained by the surface magnetic field. Some forward electrons that can overcome the surface magnetic field are transported into the target. As the electrons pass the *positive* B_z field at the front surface, they deviate from their initial (forward) direction, and are deflected to a direction between the laser propagation axis and the target surface due to the magnetic force perceived. Finally, they escape from the rear target surface, forming the rear SFE beam as shown in Fig. 1.

In a related theoretical work by Nakamura *et al.* [29], the surface magnetic field and fast electron current has also been discussed. According to their model, the fractions of the surface electrons increase with the incident angles. This agrees with our measurements. A critical angle, above which no fast electrons are injected into the target at all, is also predicted in their model. This angle, however, does not appear in our experiments. There are always some fast electrons observed behind the target. This may be due to the significant differences between the real experimental conditions and the simple assumptions used in the model such as infinite laser and electron beam diameters, etc.

To find out the generation conditions for the SFE beam, *s*-polarized and circularly-polarized laser pulses, as well as different target materials (CH and Al), were also applied at different laser incident angles in the experiments, respectively. The results were similar to those shown in Fig. 1. To check the role of the electron density scale length, a prepulse with a duration of 200 ps, split from the main beam before the compressor, was used to create a preplasma. The separation between the prepulse and the main pulse was ~0.5 ns. The size of the prepulse focal spot was ~20 μm in diameter. The laser intensity for the main pulse was set to be 1–2 $\times$ 10^{18} W/cm^2, similar to that in Fig. 1. Figure 4(a) shows the angular distributions of fast electrons with and without a 36 mJ prepulse at an incident angle 60°. The emission peak shifts to the laser specular direction and the electron number close to the front target surface decrease almost to the noise level after introducing the prepulse. Figure 4(b) shows the results for three different prepulse energies at an incident angle 45°. The surface fast electron emission is affected only slightly when using the smallest prepulse energy 4 mJ. However, when increasing the prepulse energy further, the surface

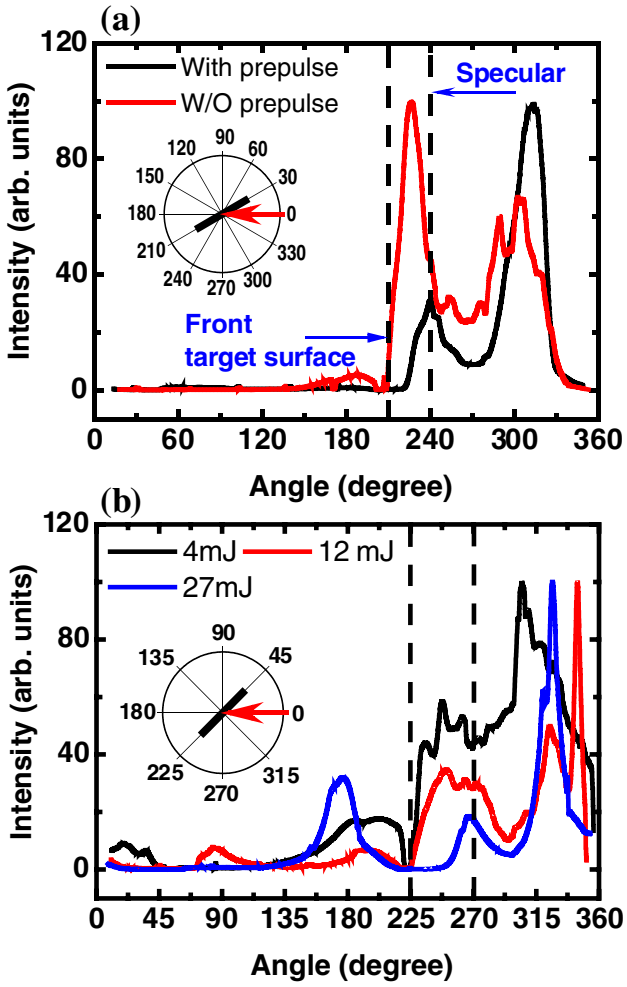

FIG. 4 (color online). (a) Angular distributions of fast electrons with and without a prepulse at the incident angle 60°. (b) Angular distributions for different prepulse energies at the incident angle 45°.

electron emission switches to the laser specular direction gradually. For the prepulse energy 27 mJ, the peak has fully shifted to the specular direction. The electron number close to the surface also decreases to zero, accordingly.

Similarly, in our PIC simulations, when a large scale preplasma was added in front of the sharp-boundary plasma slab, surface fast electrons were not observed either. The experimental and simulation results suggest that strong quasistatic surface magnetic and electric fields are essential to the formation of the SFE beam. A large scale preplasma will spoil the formation of large surface fields and lead to disappearance of the SFE beams. In our experiments the energy of the intended prepulse must be lower than $\sim$10 mJ in order to observe the surface electron beams.

Note the SFE beam survives for a small scale preplasma in the experiments [see Fig. 4(b)]. This is because the density of the laser turning point (where the light wave is reflected), $n_{tp} = n_{cr}\cos^2\theta$, where n_{cr} and θ are the critical density and the angle of incidence, respectively, becomes small for large incident angles. For instance, for $\theta = 45°$ $n_{tp} = 0.5n_{cr}$. This leads to the effect that the preplasma is much reduced for large incident angles.

In summary, we have observed a novel fast electron beam propagating along the target surface due to the confinement of the quasistatic magnetic and electric fields. The SFE beam can be used as a laser-based electron source with an ultrashort pulse length (about ps) for applications. Our results also support the viewpoint that a reentrant cone in fast ignition experiments can guide fast electrons along the conical inner surface to the compressed target region.

This work was supported by the NSFC (Grants No. 10374115, No. 60321003, No. 10510490, No. 10335020, No. 10425416, No. 10334110, and No. 10390161), the National High-Tech ICF program, and National Key Laboratory of High Temperature and High Density Plasma.

*To whom correspondence should be addressed.
Electronic address: jzhang@aphy.iphy.ac.cn

[1] M. H. Key *et al.*, Phys. Plasmas **5**, 1966 (1998).
[2] J. R. Davis *et al.*, Phys. Rev. E **56**, 7193 (1997).
[3] A. R. Bell *et al.*, Phys. Rev. Lett. **91**, 035003 (2003).
[4] M. Borghesi *et al.*, Phys. Rev. Lett. **83**, 4309 (1999).
[5] L. Gremillet *et al.*, Phys. Rev. Lett. **83**, 5015 (1999).
[6] M. Honda *et al.*, Phys. Plasmas **7**, 1302 (2000).
[7] S. Wilks *et al.*, Phys. Plasmas **8**, 542 (2001).
[8] S. Hatchett *et al.*, Phys. Plasmas **7**, 2076 (2000).
[9] M. Allen *et al.*, Phys. Rev. Lett. **93**, 265004 (2004).
[10] J. Fuchs *et al.*, Phys. Rev. Lett. **94**, 045004 (2005) and references therein.
[11] H. Schwoerer *et al.*, Phys. Rev. Lett. **86**, 2317 (2001).
[12] K. W. D. Ledingham *et al.*, Science **300**, 1107 (2003).
[13] M. Tabak *et al.*, Phys. Plasmas **1**, 1626 (1994).
[14] R. Kodama *et al.*, Nature (London) **412**, 798 (2001).
[15] R. Kodama *et al.*, Nature (London) **418**, 933 (2002).
[16] Y. Sentoku *et al.*, Phys. Plasmas **11**, 3083 (2004).
[17] Z. L. Chen *et al.*, Phys. Rev. E **71**, 036403 (2005).
[18] R. Kodama *et al.*, Nature (London) **432**, 1005 (2004).
[19] P. A. Norreys *et al.*, Phys. Plasmas **11**, 2746 (2004).
[20] S. D. Baton *et al.*, Plasma Phys. Controlled Fusion **47**, B777 (2005).
[21] K. A. Tanaka *et al.*, Rev. Sci. Instrum. **76**, 013507 (2005).
[22] Z.-M. Sheng *et al.*, Phys. Rev. Lett. **85**, 5340 (2000).
[23] Y. T. Li *et al.*, Phys. Rev. E **64**, 046407 (2001).
[24] S. Bastiani *et al.*, Phys. Rev. E **56**, 7179 (1997).
[25] R. Tommasini *et al.*, Appl. Phys. B **79**, 923 (2004) even observed fast electrons emitted along the target surface irradiated by short laser pulses at normal incidence. The underlying physics is still unclear.
[26] A. Pukhov *et al.*, Phys. Plasmas **6**, 2847 (1999).
[27] C. Gahn *et al.*, Phys. Rev. Lett. **83**, 4772 (1999).
[28] M. Chen *et al.* Opt. Express **14**, 3093 (2006).
[29] T. Nakamura *et al.*, Phys. Rev. Lett. **93**, 265002 (2004).